Heliyon 10 (2024) e39334

Contents lists available at ScienceDirect

Heliyon

journal homepage: www.cell.com/heliyon

Research article

Filamin B knockdown impairs differentiation and function in mouse pre-osteoblasts via aberrant transcription and alternative splicing

Xi Wang [a,b,c,1], Qiyu Jia [b,1], Li Yu [d,1], Jinyong Huang [b], Xin Wang [b], Lijun Zhou [e], Wubulikasimu Mijiti [b], Zhenzi Xie [f], Shiming Dong [b], Zengru Xie [b,**], Hairong Ma [a,b,c,*]

[a] State Key Laboratory of Pathogenesis, Prevention and Treatment of High Incidence Diseases in Central Asia, Clinical Medicine Institute, The First Affiliated Hospital of Xinjiang Medical University, Urumqi 830011, Xinjiang, China
[b] Xinjiang Clinical Research Center for Orthopedics, Urumqi, 830011, Xinjiang, China
[c] Key Laboratory of High Incidence Disease Research in Xinjiang Medical University, Ministry of Education, Urumqi, 830011, Xinjiang, China
[d] Department of Integrated Cardiology, The First Affiliated Hospital of Xinjiang Medical University, Urumqi, 830000, China
[e] School of Public Health, Xinjiang Medical University, Urumqi, 830011 Xinjiang, China
[f] School of Basic Medicine, Xinjiang Medical University, Urumqi, 830011 Xinjiang, China

ARTICLE INFO

Keywords:
Filamin B
MC3T3-E1
Alternative splicing
RNA-Sequencing

ABSTRACT

Objective: Filamin B (FLNB) encodes an actin-binding protein that is known to function as a novel RNA-binding protein involved in cell movement and signal transduction and plays a pivotal role in bone growth. This study aimed to investigate possible FLNB function in the skeletal system by characterizing the effecs of FLNB knockdown in mouse preosteoblast cells.
Methods: Stable FLNB MC3T3-E1 knockdown cells were constructed for RNA-seq and alternative splicing event (ASE) analysis of genes involved in osteoblast differentiation and function that may be regulated by FLNB. Standard transwell, MTT, ALP, qPCR, Western blot, and alizarin red staining assays were used to assess functional changes of FLNB-knockdown MC3T3-E1 cells.
Results: Analysis of differentially expressed genes (DEGs) in FLNB knockdown cells revealed enrichment for genes related to osteoblast proliferation, differentiation and migration, such as ITGA10, Cebpβ, Grem1, etc. Alternative splicing (AS) analysis showed changes in the predominant mRNA isoforms of skeletal development-related genes, especially Tpx2 and Evc. Functional asslysis indicated that proliferation, migration, and differentiation were all inhibited upon FLNB knockdown in MC3T3-E1 cells compared to that in vector control cells.
Conclusions: FLNB participates in regulating the transcription and AS of genes required for osteoblast development and function, consequently affecting growth and development in MC3T3-E1 cells.

* Corresponding author. State Key Laboratory of Pathogenesis, Prevention and Treatment of High Incidence Diseases in Central Asia, Clinical Medicine Institute, The First Affiliated Hospital of Xinjiang Medical University, Urumqi, 830011, Xinjiang, China.
** Corresponding author.
E-mail addresses: xiezenru@126.com (Z. Xie), mahr@xjmu.edu.cn (H. Ma).
[1] Xi Wang, Qiyu Jia and Li Yu contributed equally to this study.

https://doi.org/10.1016/j.heliyon.2024.e39334
Received 3 July 2024; Received in revised form 11 October 2024; Accepted 11 October 2024
Available online 12 October 2024

1. Introduction

Osteoporosis (OP) is a systemic disease of bone metabolism characterized by a pathological decrease in bone density and volume due to dysregulation of several contributing factors, leading to deterioration of the bone microstructure, increased bone fragility, and susceptibility to fracture [1]. While OP has a prevalence of 4–6% among people over 50 years of age in Europe and the United State [2], its prevalence exceeds 15 % in this age group in Asia [3]. OP has thus emerged as a major public health concern due to the rapidly increasing size of the aging demographic. Osteoporotic fracture is the most devastating consequence of OP and is accompanied by increased morbidity and mortality [1].

However, fundamental research investigating the molecular mechanisms leading to OP remains limited. Additionally, therapeutic options for OP show relatively unsatisfactory efficacy, including significant side effects and limited benefits in reversing OP progression [4]. Hence, therapeutic development to improve outcomes for OP patients requires more effective molecular targets.

Among potential target involved in osteoblast development, filamins comprise a large family of dimer-forming actin-binding proteins [5]. In particular, Filamin B (FLNB), which contains two calpain homologous domains and a rod-like domain composed of 24 homologous repeats, mediates linkage of the actin cytoskeleton to form a dynamic structure [6]. It has also been shown to immobilize the cytoskeleton to membrane-bound plasma adhesion receptors [7]. Clinical evidence suggests that mutations in FLNB can cause the occurrence of multiple skeletal disorders, such as vertebral-carpal fusion sign, adolescent idiopathic scoliosis, and Larsen's syndrome in the fetal period [8–10].

Other studies have shown that FLNB is involved in the progression of osteoporosis and is a susceptibility gene that regulates bone density [11]. Recently, UV cross-linking of modified nucleosides with affinity purification conducted by Baltz et al. revealed that FLNB can also function as an RNA-binding protein (RBP) to form complexes with mRNAs [12]. Other RBPs have been found to perform pivotal roles in the formation and function of transcripts and maintenance of cellular homeostasis [13,14]. FLNB also reportedly participates in post-transcriptional regulation of RNA metabolism, including RNA splicing, polyadenylation, localization, translation, and degradation [15]. However, it remains unclear whether the RBP functions of FLNB are also involved in regulating the pathogenesis of OP.

The objective of this study was to explore the potential role of FLNB in regulating the transcription of genes required for skeletal development and to identify its downstream targets involved in osteoblast proliferation, differentiation and angiogenesis. We hypothesized that FLNB may regulate genes required for osteoblast development and/or Alternative Splicing Events (ASEs) that may regulate osteoblast proliferation, differentiation and angiogenesis. Our results provide new insights into FLNB function in osteoblasts

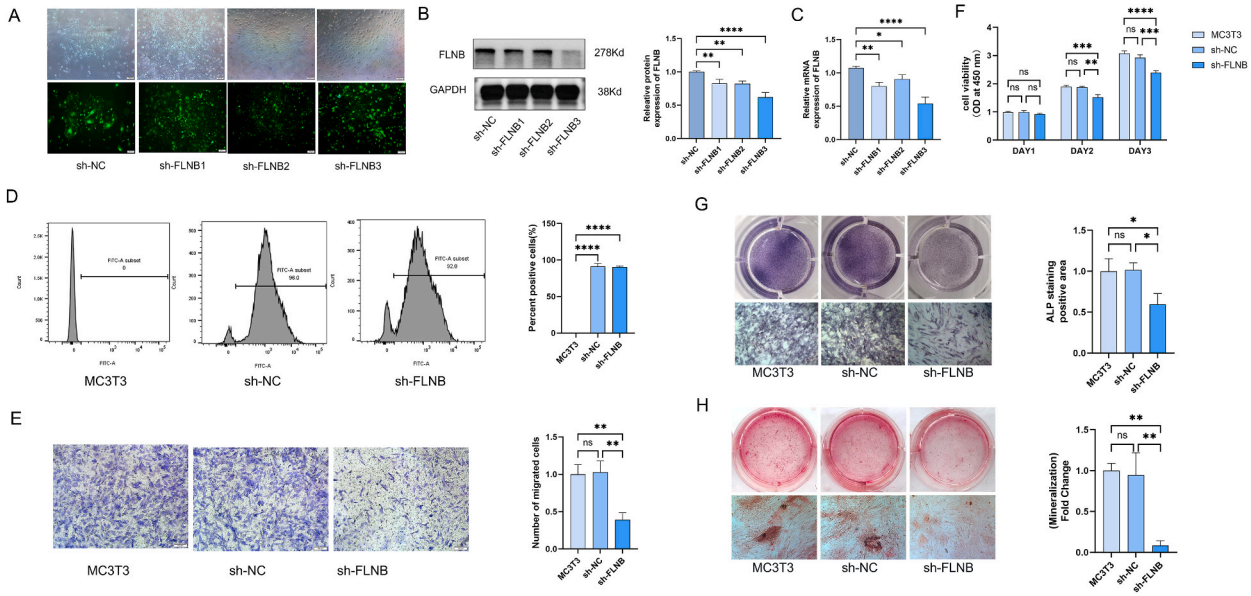

Fig. 1. Reduced proliferation, migration, and differentiation following FLNB knockdown in MC3T3 cells.
A) Green fluorescence protein (GFP) expression in lentivirus-infected MC3T3-E1 cells. B) Western blots (left) and quantitative band density analysis (right) of FLNB expression in cells with knockdown by three independent shRNA constructs or sh-NC vector controls. C) RT-qPCR analysis of FLNB transcript levels in MC3T3 cells expressing three independent shFLNB RNAs or sh-NC controls. D) Flow cytometry analysis of MC3T3 cells expressing no shRNAs (left), sh-NC (middle left), or sh-FLNB (middle right), and statistical summary of positively infected cells (right). E) Transwell migration assays of MC3T3-E1 cells with or without FLNB knockdown (left) with quantitative analysis (right). F) MTT assays of proliferative capacity in MC3T3 cells with or without FLNB knockdown. G) ALP assays of osteogenic differentiation capacity in MC3T3 cells with or without knockdown of FLNB. H) Alizarin red staining assays of osteogenic differentiation MC3T3 cells with or without knockdown of FLNB. Significant differences between groups were determined by *t*-test. Data represent means±SD of three independent experiments; *P < 0.05; **P < 0.01; ***P < 0.001; ****P < 0.0001; ns indicates no significance.

and suggest new potential therapeutic targets that warrant further exploration for gene-based stem cell therapies of OP.

2. Materials and methods

2.1. MC3T3-E1 stable cell line cell culture and knockdown of FLNB

Mouse cranial parietal osteogenic precursor cells (MC3T3-E1, MC3T3) were obtained from Procell (Wuhan, China) were used and cultured in α-MEM (Gibco, Thermo, USA). MC3T3 cells were infected with lentivirus carrying shRNA_FLNB or an empty vector following the protocols provided by Yuanjing Biologicals (China). Prior to knockdown, three independent shRNA sequences were compared for FLNB silencing efficiency, including shRNA_FLNB1 (5′-GCCGACATTGAAATGCCGTTT-3′), shRNA_FLNB2 (5′-CCCACA-TACGATGCAAGCAAA-3′), and shRNA_FLNB3 (5′-GCTGGAAACTACA GGGA ACAT-3′) (see Fig. 1).

MC3T3 cells with good growth status were inoculated in six-well plates at a cell density of 1×10^5 cell/well culturing in complete medium (composed of 90 % α-MEM, 1 % penicillin/streptomycin and 10 % FBS). After 24 h, 1 ml of complete medium containing 5ug/ml Polybrene and 20ul of virus with a viral titer of 1×10^8 TU/ml was added. After another 24 h, the original medium was removed and replaced it with fresh one. Green fluorescence was observed 48–72 h later using a fluorescence microscope. Additionally, the cells were screened with a complete medium containing 5ug/ml puromycin for 7 d, after which they were maintained in a complete medium containing 2.5ug/ml puromycin.

2.2. Flow cytometry assay

Flow cytometry analysis carried GFP fluorescent probe to screen positive cells infected with specific lentivirus. The cell precipitates of MC3T3 (blank), sh-NC (empty vector) and sh-FLNB (knockdown group) were collected and incubated at 37 °C for 48 h. The number of cells in each group was more than 1×10^5. The collected living cells were washed twice with cold 1 × PBS, and then the cells were filtered using a 200-mesh cell filter. Flow cytometry (Beckman, USA) was used for detection.

2.3. Methyl thiazolyl tetrazolium assay (MTT) and transwell assay

MC3T3, sh-NC and sh-FLNB cells were inoculated in 96-well plates at a density of 5×10^3 cells per well. After 24, 48 and 72 h of cell culture, the MTT working solution was added and incubated at 37 °C for 1 h. The absorbance of the solution was measured at a wavelength of 450 nm using a spectrophotometer.

Transwell was utilized to assess the migration abilities of MC3T3 cells. The pre-starved cells were digested with trypsin, resuspended, and washed with phosphate buffer saline (PBS, Servicebio, China). Then, 1×10^5 cells per well were resuspended in a basic α-MEM (Gibco, USA) medium and 200 μl of the cell solution was added to the upper chamber. Additionally, 600 μl of complete medium containing 10 % FBS was added to the lower chamber. After 24–48 h of incubation in a 37 °C incubator, the culture medium was discarded and the cells were washed twice with PBS. The cells were fixed with 4 % paraformaldehyde for 30 min, rinsed with PBS 3 times, and stained with 0.2 % crystal violet (filtered through a microporous membrane before use) for 30 min. After being washed with PBS 2–3 times, the cells were observed under an inverted microscope and pictures were taken.

2.4. Alkaline phosphatase (ALP) staining assay

MC3T3, sh-NC, and sh-FLNB cells were inoculated into 12-well plates at 2×10^4 cells per well. When the cell fusion rate reached 80 %, an osteogenic induction solution was added to induce differentiation. Seven days after induction, cells were removed and washed three times with PBS. The cells were fixed at room temperature for 10 min, using 4 % paraformaldehyde solid, stained according to the instructions based on the alkaline phosphatase kit, and the staining was observed under a microscope and photographed.

2.5. Alizarin red staining (ARS) assay

MC3T3, sh-NC and sh-FLNB group cells were inoculated into 6-well plates at 5×10^4 cells/well density and cultured. After 24 h, the medium was changed to one containing an osteogenic induction solution. The fresh induction medium was changed every 3 days, and after 21d of osteogenic induction, the cells were fixed using 4 % paraformaldehyde for 15 min and rinsed in ddH_2O. We removed the 6-well plate and stained the wells with 1 % Alizarin Red S (pH 4.2) for 30 min at room temperature, observed the samples under a light microscope, and took representative photographs.

2.6. RNA sequencing (RNA-seq) library and differentially expressed genes (DEGs) analysis

Approximately 1×10^5 cells expressing sh-NC or sh-FLNB were inoculated into each well of a six-well plate (three wells per group). After cells grew to confluence (on day 3 post inoculation), the cell precipitates were collected for bulk RNA-seq using three replicates per group. Total RNA was extracted according to the TRIzol® (Invitrogen, Thermo, USA) kit instructions. RNA sequencing libraries were created from each sample using the AHTS Stranded mRNA Sequencing Library Prep Kit (Vazyme Biotechnology Ltd.) and 1 μg of total RNA. The cDNA libraries were created following manufacturer's instructions and processed by the Ilumina Novaseq 6000 system for 150 nt paired-end sequencing. RNA-seq cDNA libraries of sh-FLNB group and sh-NC group cells were constructed. After removing

aptamers and low-quality base reads, the resulting nucleotide-paired raw reads were compared to the mouse genome (GRCm39) group using TopHat2. By using the unique mapped reads, FPKM was used to assess normalized transcript levels.

Adaptors were eliminated from the raw reads through using Cut adapt, while the FASTX-Toolkit was employed for the trimming of low-quality bases [16]. Next, gene expression levels were determined using FPKM, calculated as: FPKM = total exon fragments/(uniquely mapped reads*exon length), and differential expression analysis was conducted using DESeq2 [17]. Differentially expressed genes (DEGs) were screened using fold change (FC)≥2 or ≤1/2 with a significance level of $P < 0.01$ as a threshold. Furthermore, Pearson correlation analysis was employed to evaluate the correlation between samples. GO determined the functional categories of DEGs. With the KOBAS 2.0 server, the top 10 items with the highest enrichment were selected and drawn.

2.7. Alternative splicing (AS) analysis

The significance threshold for identifying significantly different alternative splicing events (ASEs) was set at $p \leq 0.05$. The ABLas pipeline analyzes, quantifies, and regulates ASEs between samples. The occurrence of ASE is checked by splice junction reads and unique mapping reads. ASEs consist of exon jumps (ES), alternative 3'splice sites (A3SS), intron retention, alternative 5'splice sites (A5SS), mutually exclusive exons (MXE), mutually exclusive 3′untranslated regions (UTRs), mutually exclusive 5′ UTRs, cassette exons, A3SS&ES, and A5SS&ES. ASE significantly below the FDR ≤5 % threshold was classified as RBP-regulated ASE [18].

2.8. Reverse transcription and real time quantitative PCR (RT-qPCR)

MC3T3 cells expressing sh-NC or sh-FLNB were inoculated into 6-well plates at a density of 1×10^5 cells/well. At 48 h post inoculation, cells were collected for RNA extraction. The knockdown efficiency of the FLNB was evaluated through RT-qPCR. Furthermore, RT-qPCR was used to verify the results of DEG and AS. RNA was extracted using the TRIzol® kit (Thermo Fisher, USA) and cDNA synthesis was performed following the standard protocol (Servicebio, China). RT-qPCR was performed on the ABI QuantStudio 5, followed by denaturing at 95 °C for 10 min, 40 cycles of denaturing at 95 °C for 15 s and annealing and extension at 60 °C for 1 min. Each sample had three technical replicates. Data was analyzed using the comparison Cq ($2^{-\Delta\Delta Cq}$) method [19]. The primer sequences are listed in Table 1.

Alternative splicing events (ASEs) were validated by RT-qPCR assays using a reverse primer that targeted the constitutive exon paired with forward primers that spanned the boundary between the constitutive or alternative exons in order to detect normal or alternative splicing transcripts (see Table 1 for a complete list of primers used in this study). The proportion of alternatively spliced transcript isoforms was calculated as follows: alternative splicing transcripts/(variable splicing transcript + normal template transcript), and this ratio was then compared between samples. The primer sequences are listed in Table 2.

2.9. Western blot

The cells in the sh-NC and sh-FLNB groups were lysed using RIPA buffer (Solaribio, China). The supernatants collected from the samples were subjected to protein concentration determination using the BCA Protein Concentration Assay Kit (Thermo Scientific, USA). The proteins from sh-NC and sh-FLNB groups were electrophoresed on 10 % polyacrylamide gels and then transferred to PVDF

Table 1
Primer sequence information.

Gene (DEG)	Sequence (5'→3')
Cebpb	FORWARD:AGCTGAGCGACGAGTACAAGATG
	REVERSE:TTGTGCTGCGTCTCCAGGTTG
Ccdc85b	FORWARD:AGGAGCTGACGGACGAGGAG
	REVERSE:GGTCCCAAAGAGCTGCCACTG
Grem1	FORWARD:CGCACTATCATCAACCGCTTCTG
	REVERSE:TTTCTTCTTGGTGGGTGGCTGTAG
Ctsh	FORWARD:GTCCTGGCGGTTGGCTATGG
	REVERSE:GAGGAATGGGATAGGAGGCACAAG
Sphk1	FORWARD:AGAGTGCTGGTGCTGCTGAAC
	REVERSE:TGGTTCTTCCGTTCGGTGAGTATC
Col6a2	FORWARD:CTGAGCGTGCCCGTGAAGAG
	REVERSE:CTTGATGATGCGGTTGATGGTGTC
Cleclla	FORWARD:CCTICTTCTAGTCCCAACCCTTTCC
	REVERSE:GGTGTCACTCGCAGCATCCC
Col6a3	FORWARD:AACTGATGGACAATCGGAGGATG
	REVERSE:AGTGGTTCGCTIGCTACTICTCC
ITGA10	FORWARD:TGTGAGAGCAGCAAGGAACCTAA
	REVERSE:TCCATCAGTGACAACTACCAGCAG
Nrp2	FORWARD:CATCTCCTCAGGCTCCGTGTTATAC
	REVERSE:TGTGTGGATACTICTCIGGAAACC
Cavin4	FORWARD:CCAGTGCCGCTCCCICAAAG
	REVERSE:ACGCCCATCCCTCTGTCTACC

Table 2
As primer sequence information.

Genes (AS)	Sequence (5'→3')
Epb41l2-M-F	TGAGGGAAAGAGTTCACATG
Epb41l2-AS-F	ACCACAAGCGAGTTCACATG
Epb41l2-M/AS-R	CTCCACCTTACGAGTCTCCC
Ppm1b-M-F	CAATGATGGGATGGCAGACT
Ppm1b-AS-F	CCTATTATGAATGGCAGACT
Ppm1b-M/AS-R	GTGGAATGCTCGACTCGTTT
Mbd1-M-F	GGACGAGCTAAAGCGGCTGC
Mbd1-AS-F	GTTTGCCATGAAGCGGCTGC
Mbd1-M/AS-R	TGGAGTTGTCGAGCAGAAGC
Tpx2-M-F	TGTATACATGAAGACAGTCT
Tpx2-AS-F	AGGTTGTCAGAAGACAGTCT
Tpx2-M/AS-R	TATCCTCTTCAGCATCCAAA
Evc-M-F	GTAGGTTGTACTGAGTGGTC
Evc-AS-F	CCTTCCGCCGCTGAGTGGTC
Evc-M/AS-R	GAACCAAAAGGAAGAAACCC
Rtkn-M-F	GTCGCCGGAGGACACAGAGC
Rtkn-AS-F	CAGCCTGGAGGACACAGAGC
Rtkn-M/AS-R	GTAGCTGAGAATACGGCTGTTG

membranes. Subsequently, these were incubated for 2 h at room temperature with 5 % (w/v) skim milk powder. Then, the membrane was incubated with the appropriate antibody concentration at 4 °C overnight (FLNB, 1:1000, Proteintech; CEBP/β,1:1000, Affitiny; GREM1,1:1000, Affitiny; ITGA10,1:1000, Affitiny; GAPDH,1:5000, Proteintech). After incubation, the membrane was washed with TBST. Subsequently, the membrane was incubated with goat anti-rabbit secondary antibody (1:5000, Proteintech, China) for 1 h at room temperature [20]. The gray value of each band was quantitatively analyzed using ECL chemiluminescence and ImageJ 1.46 r software.

2.10. Statistical analysis

Independent sample *t*-test was used for comparison between the two groups, and one-way ANOVA was used for comparison between multiple groups. $P < 0.05$ was considered statistically significant. The results of the experiment were recorded as the mean ± SEM of three replicates. Data were analyzed using Prism software version 9.5 (GraphPad, USA).

3. Results

3.1. FLNB regulates the migration, proliferation and differentiation in MC3T3 cells

To investigate the effects of FLNB on osteoblast function, we induced stable FLNB knockdown by infecting MC3T3-E1-E1 cells with lentivirus carrying sh-FLNB1, sh-FLNB2, sh-FLNB3 or an shRNA-scramble (sh-NC) vector control. After confirming GFP expression by microscopy at 48 h post infection (Fig. 1A), Western blots and rt-qPCR assays indicated FLNB protein and mRNA levels were significantly lower in cells expressing sh-FLNB3 compared to that in sh-FLNB1, sh-FLNB2, and the sh-NC controls groups (Fig. 1B and C; $P < 0.05$). Based on these results showing the strongest knockdown efficiency, cells expressing sh-FLNB3 (sh-FLNB, hereafter) were selected for all subsequent experiments. Subsequent flow cytometry assays to quantify infection efficiency showed that the virus was stably maintained in more than 90 % of the MC3T3 population (Fig. 1D; $P < 0.05$), suggesting that knockdown levels were sufficiently high to allow further characterization of FLNB function.

Transwell assays of cell migration capability indicated that significantly fewer sh-FLNB cells could penetrate the empty chamber compared to wild-type MC3T3 (WT) and sh-NC cells, while the sh-NC group showed no significant difference from WT (Fig. 1E; $P < 0.05$), suggesting that decreased FLNB expression could impair migration in these osteogenic precursor cells. Subsequent MTT assays further showed that proliferation decreased with time in sh-FLNB cell cultures, whereas both sh-NC and uninfected WT cells both showed gradually increasing proliferation over time (Fig. 1F; $P < 0.05$). These results suggested that FLNB suppression could inhibit proliferation in MC3T3 cells.

Given these functional effects of FLNB knockdown, we next assessed the impacts of FLNB knockdown on osteogenic differentiation by treating each group with an osteogenic induction solution for 7 days. ALP activity assays conducted in the early stages of osteogenic differentiation showed that the sh-FLNB group had lower ALP activity than that of either the sh-NC or MC3T3 groups (Fig. 1G; $P < 0.05$). At 21 days after inducing osteogenesis, alizarin red staining similarly showed that sh-FLNB cells had less calcium deposition than either WT or sh-NC cells (Fig. 1H; $P < 0.05$), which had comparable calcium deposition levels. These results suggested that FLNB was required for function and osteogenic differentiation in MC3T3 cells.

3.2. FLNB knockdown leads to differential expression of multiple osteoporosis-associated genes in MC3T3-E1 cells

After confirming FLNB transcriptional knockdown by RNA-seq analysis (Fig. 2A; $P < 0.05$), we next analyzed the FPKM values of

27,456 total genes detected in the sh-FLNB and sh-NC MC3T3-E1 cells to identify genes involved in FLNB function. In total, DEseq2 identified 317 total DEGs between the sh-FLNB and sh-NC cells ($|FC| \geq 2$ or ≤ 0.5, $P < 0.01$), including 113 up-regulated and 204 down-regulated DEGs (Fig. 2B–Table 3). GO functional annotations showed that these 113 significantly upregulated DEGs were enriched in terms related to angiogenesis, apoptosis, cell differentiation, and other related processes (Fig. 2C). Among the top 40 up-regulated genes ranked by FPKM, we noted that Coiled-coil domain containing 85B (Ccdc85b), Gremlin1 (Grem1), CCAAT enhancer binding protein (C/EBPβ), Cathepsin H (Ctsh), and sphingosine kinase 1 (Sphk1) were enriched in pathways of angiogenesis, apoptosis and cell differentiation, the latter three of which are known to play a role in the progression of bone diseases. In contrast, GO analysis revealed that the 204 down-regulated DEGs in sh-FLNB cells were mainly enriched in processes related to cell adhesion, proliferation, differentiation, and extracellular matrix tissue (Fig. 2C). It is worth noting that the osteoporosis-associated genes type VI collagen α chain 2 (Col6a2), type VI collagen α chain 3 (Col6a3), C-type lectin domain family 11 member A (Clec11a), integrin subunit α10 (ITGA10), Neuropilin-2 (NRP2), and Cavin4 were all among the 40 most down-regulated genes based on FPKM.

RT-PCR confirmed the differential expression. As a result, these findings show a strong correlation between the results of the FLNB knockdown and the RNA-seq data, suggesting the reliability of the FLNB-regulated DEG identified from the RNA-seq analysis (Fig. 3A and B; $P < 0.05$). In agreement with the RNA-seq results, WB analysis further revealed that ITGA10 protein levels were significantly lower in the sh-FLNB group, while GREM1 and CEBP/β levels were significantly higher compared with that in MC3T3-E1 cells expressing the sh-NC control virus. These findings further supported the likelihood that FLNB functioned as a regulator of multiple bone development-related genes (Fig. 3C; $P < 0.05$).

3.3. *FLNB knockdown leads to changes in AS of genes involved in bone development in MC3T3 cells*

Given previous reports of FLNB function as an RBP involved in post-transcriptional regulation via AS[21], we next screened our RNA-seq data for differential ASEs associated with FLNB knockdown in MC3T3-E1 cells. In total, we detected 612 ASEs that showed significant differential splicing ratios between FLNB knockdown and vector control groups, including 277 up-regulated and 335 down-regulated ASEs (Fig. 4A; Table 4). GO analysis of genes with differential ASEs in FLNB knockdown cells showed enrichment in pathways involved in regulation of transcription by 'regulation of RNA polymerase II', 'cellular response to DNA damage stimuli', 'DNA repair', 'positive regulation of cell adhesion', 'cell division' and others (Fig. 4B). The present results identified that there were only four DEGs with significantly altered splicing including Ccdc80, Sned1, Col18a1 and Ccn5 (Fig. 4C). Notably, demonstrated changes in expression and AS after FLNB knock-down (Fig. 4D). In line with our above AS assays, subsequent RT-qPCR analysis indicated that the Evc gene had a lower ratio of AS transcripts in sh-FLNB cells relative to that in sh-NC control cells. By contrast, Epb41l2 and Ppm1b had higher ratios of AS transcripts in FLNB knockdown cells compared to sh-NC controls. In addition, ratios of Mbd1 and Rtkn AS transcripts showed no significant difference between groups while, unexpectedly, the proportion of Tpx2 AS transcripts was higher under FLNB knockdown than that in control cells.

4. Discussion

In this study, we investigated the transcriptomic and functional effects of FLNB expression on osteoblast growth and development

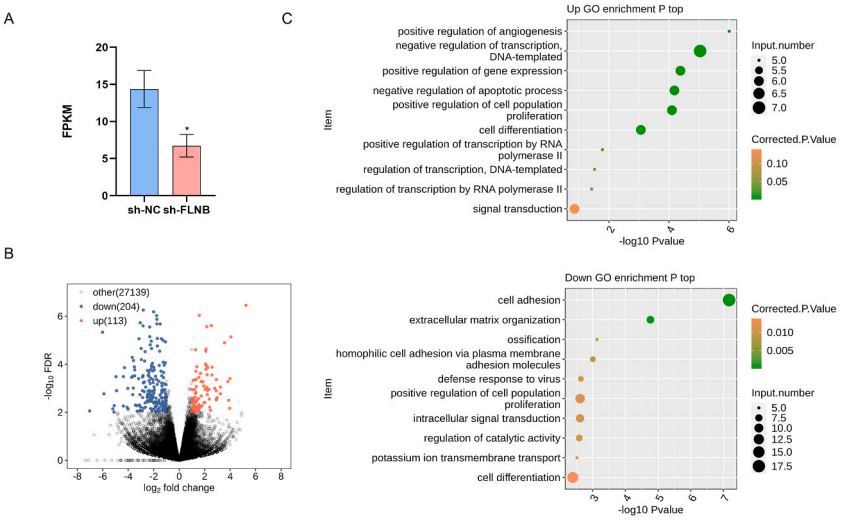

Fig. 2. RNA-seq analysis of sh-FLNB regulated gene expression.
A) RNA-seq was used to compare the FLNB expression levels of sh-FLNB and sh-NC. *$P < 0.05$. B) Volcano plots show DEGs by sh-FLNB and samples in each group were compared to control cells. The red color indicates up-regulated genes ($log_2FC \geq 1$, $P < 0.01$) and the blue color indicates down-regulated genes ($log_2FC \leq -1$and $P < 0.01$). C) GO analysis of up-regulated and down-regulated DEGs between sh-FLNB and sh-NC.

Table 3
Total number of differentially expressed genes.

DEG group	Total genes	Up regulated gene	Down regulated gene	Total
sh-FLNB vs sh-NC	27456	113	204	317

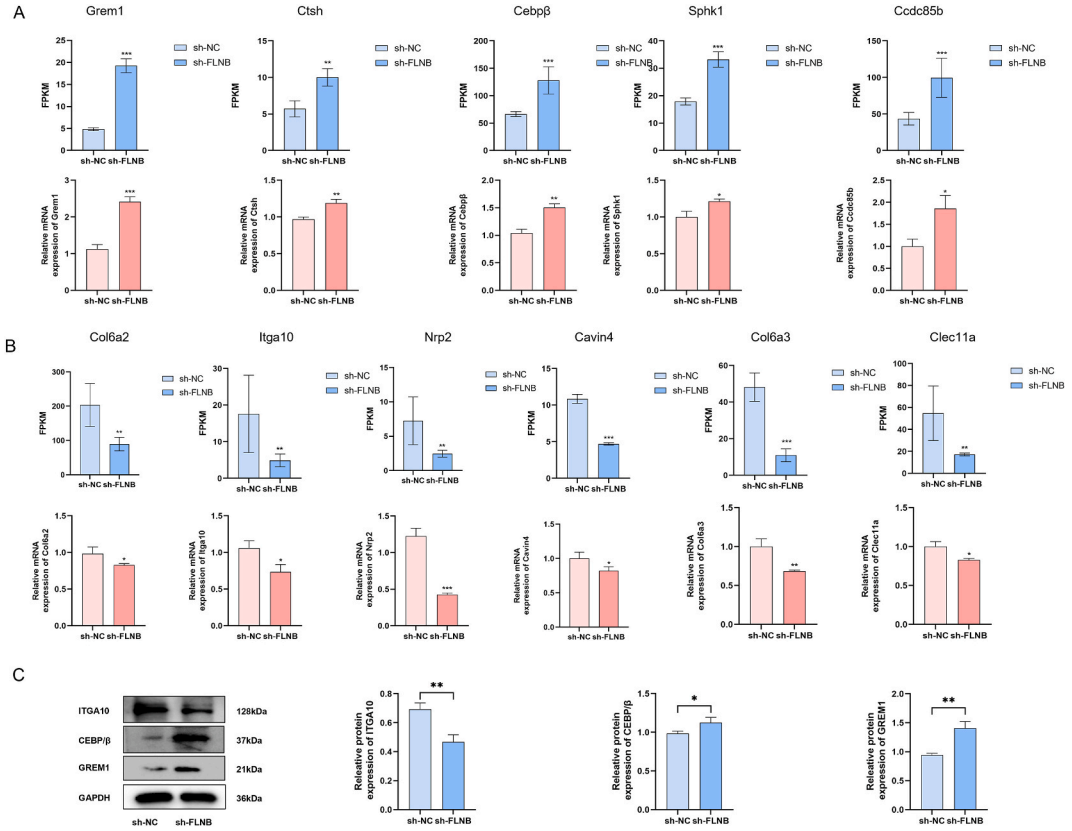

Fig. 3. Validation of FLNB-regulated genes (DEGs). A) Expression levels of osteogenesis related up-regulated DEG after knockdown of FLNB (FPKM, up) and RT-qPCR measurements (down). B) Expression levels of osteogenesis-associated down-regulated DEG after knockdown of FLNB (FPKM, up) and RT-qPCR measurements (down). C) Protein expression levels of ITGA10, CEBP/β, and GREM1 genes. Compared with sh-NC group, *P < 0.05; **P < 0.01; ***P < 0.001; ****P < 0.0001.

using FLNB knockdown MC3T3-E1 mouse cells as a model. We found that FLNB is extensively involved in regulating the expression and ASEs of multiple osteoblast development-related genes, and impacts the mRNA and protein levels of key osteogenic factors, such as ITGA10, CEBP/β, GREM1, and regulates several biological processes, such as osteoblast proliferation, migration, and osteogenic differentiation.

Grem1, Ctsh, C/EBPβ, Sphk1 are mainly involved in skeletal growth and developmental processes, and Ccdc85-b is responsible for regulating of the cellular growth cycle [22–24]. Nrp2 is involved in angiogenesis regulation [25], and Cavin4 is involved in skeletal myogenesis [26]. Among DEGs affected by FLNB, notbly, C/EBPβ is an important CCAAT enhancer-binding protein family transcription factor that has highly conserved C-terminal DNA-binding and dimerization functional domains [27]. C/EBPβ primarily regulates the transcription of genes involved in cell proliferation, differentiation, and apoptosis [28]. In the current study, we observed that mice lacking the C/EBPβ gene had significantly slower bone development conjointly with inhibition of chondrocyte maturation and osteoblast differentiation, which supported the key role of C/EBPβ in controlling osteoblast function and regulating bone mass development [29]. Other studies have also identified different isoforms of C/EBPβ that vary DNA binding characteristics which participate in regulating bone physiology-related genes [30]. Further examination of the regulatory interactions between FLNB and C/EBPβ in osteoblasts will improve our understanding of the factors leading to impaired bone development and pathogenesis of bone disease, facilitating advances in the development of targeted therapeutics to treat osteoporosis.

Gremlin1 (Grem1) is a highly conserved, secreted protein that functions as an antagonist of signaling mediated by bone morphogenetic proteins (BMPs), and has been shown to play an essential role in regulating early embryonic development of bones and kidneys [31]. Grem1 reportedly interacts specifically with BMP-2, BMP-4, and BMP-7 to prevent binding to their respective receptors [32]. Previous reports suggest that Grem1 confers tumor suppressive function, and its overexpression could inhibit tumorigenesis in

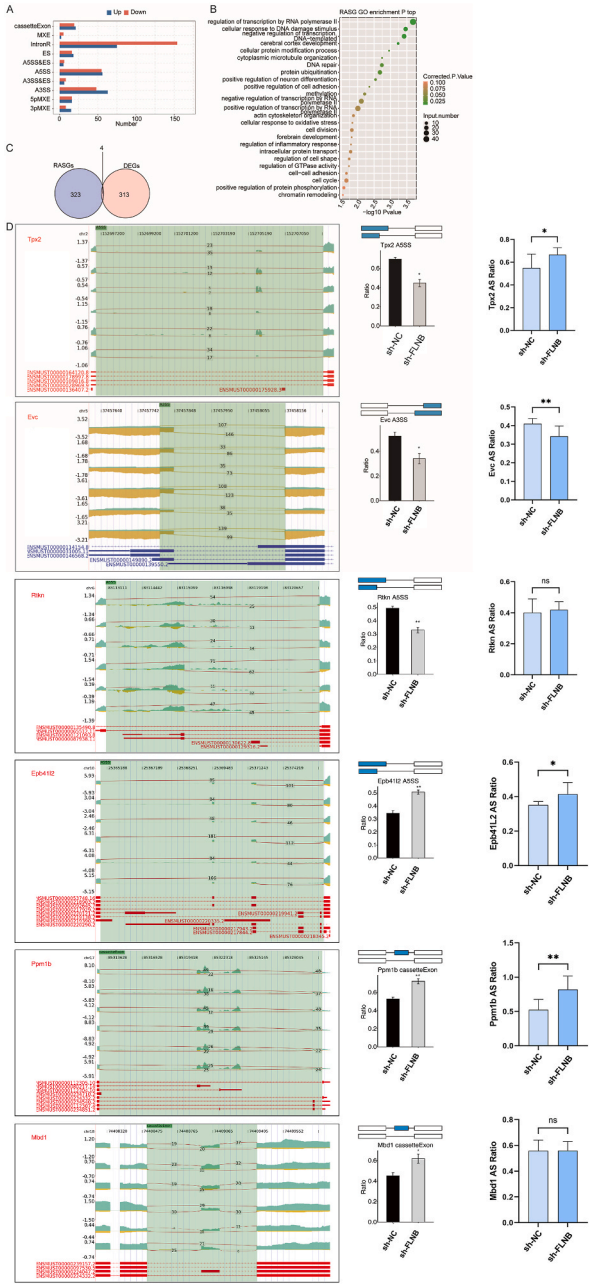

Fig. 4. Alternative splicing analysis by sh-FLNB. A) Classification of significant AS occurring of knockdown FLNB. B) GO biological process terms for regulated alternative splicing genes (RASGs) between sh-FLNB and sh-NC. C) Overlap of DEGs and RASGs. D) sh-FLNB regulates ASEs and RT-qPCR validation for Tpx2, Evc, Rtkn, Epb41L2, Ppm1b, Mbd1. Left panel: IGV-sashimi plot shows the reads distribution and splicing sites across transcript, Right panel: schematic diagram depicts the ASE structure, and barplots indicate AS ratio results from RNA-seq and RT-qPCR, respectively. Error bars represent mean ± SEM. *P < 0.05; **P < 0.01; ns indicates no significance.

DAOY neural ectoderm and Saos-2 osteoblast cell lines [33,34]. Our results show that Grem1 is upregulated upon FLNB knockdown, while proliferation and migration are decreased in MC3T3-E1 cells. These findings support the proposed critical regulatory role of Grem1 in osteoblast differentiation. It warrants mention that secreted proteins may be targeted more easily than intracellular proteins, and thus they remain a crucial source of new candidates for development of targeted therapeutics [35]. Overall, our results show an increase in Grem1 expression after FLNB knockdown. Further exploration of the specific relationship between FLNB and Grem1 may uncover more effective potential targets to treat OP.

The integrin family protein, ITGA 10, is a type II collagen-binding integrin isolated from chondrocytes [36]. Several studies have shown that ITGA10 expression is required for proliferation and differentiation of skeletal development. For instance, Liang [20] et al.

Table 4
Classification of all RASE events between sample groups.

Sample	sh-FLNB vs sh-NC	sh-FLNB vs sh-NC
Type	Up	Down
3pMXE	15	8
5pMXE	16	16
A3SS	63	48
A3SS&ES	6	8
A5SS	56	55
A5SS&ES	5	6
ES	18	16
IntronR	75	154
MXE	2	5
cassetteExon	21	19
Total	277	335

showed that ITGA10 knockdown in primary bone marrow stem cells (BMSCs) from diabetic patients could significantly reduce cell adhesion, migration, and capacity for osteogenic differentiation, while ITGA10 overexpression led to the opposite effects. In line with these observations, Song and colleagues reported that ITGA10 was significantly downregulated in osteoporosis patients, further supporting its role in osteoporosis and its normal function in promoting osteoblast development [37]. Moreover, overexpression of ITGA10 was found to activate the PI3K/AKT signaling pathway, promoting osteoblast proliferation during differentiation and inhibiting apoptosis [37]. These findings combined with our results suggest that FLNB function in regulating ITGA10 expression could partially account for the effects we observed in FLNB knockdown MC3T3-E1 cells.

AS is a fundamental mechanism of transcriptional regulation that can lead to variants in transcripts isoforms that impact protein structure and function. Interestingly, our study showed that FLNB can regulate the transcription of both normal and AS mRNA isoforms of genes involved in bone development. In FLNB knockdown cells, genes with differentially increased ASEs were mainly enriched in biological processes such as 'cell proliferation' and 'cell differentiation', as well as 'cell adhesion' and 'cell division' pathways. Our ASE analysis uncovered six transcription factors related to pre-osteoblast development with differentially increased ASEs, including Tpx2, Evc, Mbd1, IEpb41L2, and Rtkn. Previous studies have shown that Tpx2 can regulate myoblast differentiation and muscle fiber development at the transcriptome level, and interacts with tubulin to drive the cell nucleation processs [38]. Cai [39]et al. also found that myoblasts were regulated by Tpx2 in the dynamic trajectory of bovine skeletal muscle development, suggesting Tpx2 involved in skeletal muscle development. Mbd1 is involved in the development of OP by regulating the biological process of osteoblast epigenetic enzymes [40]. Evc is a positive regulator of bone growth, and its mutation can lead to maxillofacial bone dysplasia, indicating that Evc gene mutation can affect bone and cartilage dysplasia [41]. Our data showed that FLNB knockdown changed the AS pattern and inhibited the transcriptional regulation of skeletal muscle development-related genes. Therefore, the current data support the view that FLNB can regulate bone growth and development by regulating the mRNA levels of AS and bone development-related genes.

FLNB can also participate in regulating the expression of AS isoforms of genes associated with cell cycles, consequently affecting cell growth and development. For instance, the plasma membrane-associated cytoskeletal protein, IEpb41L2, plays a role in primary cilia elongation in pre-osteoblasts and promotes osteoblast differentiation [42]. The Rho effector, Rtkn, helps maintain the integrity of the microfilament cytoskeleton, providing energy for membrane transport and participating in fundamental processes of signal transduction, cell division, cell migration, immune response, etc [43]. Ppm1b is a metal ion-dependent serine/threonine protein phosphatase that has been shown to regulate cell cycle, energy metabolism, and inflammatory response through dephosphorylation of its substrates [44]. In this study, FLNB knockdown extensively altered the AS isoform levels of IEpb41L2, Rtkn, and Ppm1b, which in turn impacted the transcription of cell cycle-related genes. Future work will require further investigation of FLNB as a regulator IEpb41L2, Rtkn, and Ppm1b expression in osteoblasts.

Some limitations of this work should be noted. In this study, although we screened several key differential target genes and AS events, further verification of FLNB function is necessary using in vivo models. Future studies will also investigate the mechanism(s) of FLNB function in osteoblast growth and development in order to establish a comprehensive perspective of the regulatory role of FLNB in the process of bone remodeling.

In summary, FLNB silencing alters AS patterns for multiple genes related to MC3T3-E1 cell development, resulting in impaired proliferation, migration, and differentiation in MC3T3-E1 cells. Our findings improve our understanding of FLNB function in osteoblasts, potentially opening new possibilities for development of therapeutics that could help OP patients.

CRediT authorship contribution statement

Xi Wang: Writing – review & editing, Methodology, Data curation. **Qiyu Jia:** Writing – review & editing, Supervision. **Li Yu:** Data curation. **Jinyong Huang:** Validation. **Xin Wang:** Data curation. **Lijun Zhou:** Validation. **Wubulikasimu Mijiti:** Validation. **Zhenzi Xie:** Software. **Shiming Dong:** Validation. **Zengru Xie:** Funding acquisition. **Hairong Ma:** Writing – review & editing, Funding acquisition.

Data availability statement

data will be made available on request. The raw RNA-seq data is stored at geo@ncbi.nlm.nih.gov, user ID: 0009-0006-3349-4125.

Funding

This study was supported by the Funding District Project of the National Natural Science Foundation of China (No: 82060411; 82260409) and Xinjiang Uygur Autonomous Region Natural Science Foundation Key Projects (No: 2021D01D21; 2021D01D19).

Declaration of competing interest

The authors declare that they have no competing interests.

Acknowledgements

The funder had the following involvement with the study: study design, collection, analysis, and interpretation of data, writing the paper and decision to submit it for publication.

Abbreviations

FLNB	Filamin B
OP	Osteoporosis
RBPs	RNA-binding proteins
RT-qPCR	Real Time Quantitative PCR
RNA-Seq	RNA sequencing
DEGs	Differentially Expressed Genes
AS	Alternative splicing
FC	fold change
cDNA	Complementary Deoxyribonucleic Acid
ASEs	The alternative splicing events
ES	including exon skipping
A3SS	alternative 3′splice site;
A5SS	alternative 5′splice site;
MXEs	mutually exclusive exons
UTRs	3′untranslated regions
MTT	Methyl thiazolyl tetrazolium
GO	Gene Ontology
C/EBPβ	CCAAT enhancer binding protein; Grem1, Gremlin1
Ccdc85b	Coiled-coil domain containing 85B; Ctsh, Cathepsin; Sphk1, sphingosine kinase1
Col6a2	type VI collagen α chain2
Col6a3	type VI collagen α chain3
Clec11a	C-type lectin domain family 11 member A
ITGA10	integrin subunit α10
NRP2	Neuropilin-2
Tpx	Targeting protein for Xklp2
Evc	Ellis-van Creveld

Appendix B. Supplementary data

Supplementary data related to this article can be found at https://doi.org/10.1016/j.heliyon.2024.e39334.

References

[1] K.E. Ensrud, C.J. Crandall, Osteoporosis, Ann. Intern. Med. 167 (2017) ITC17–ITC32, https://doi.org/10.7326/AITC201708010.
[2] P.M. Camacho, et al., AMERICAN association of clinical endocrinologists/AMERICAN college of endocrinology clinical practice guidelines for the diagnosis and treatment of postmenopausal osteoporosis- 2020 update executive summary, Endocr. Pract. 26 (2020) 564–570, https://doi.org/10.4158/gl-2020-0524.
[3] Y. Jiang, P. Zhang, X. Zhang, L. Lv, Y. Zhou, Advances in mesenchymal stem cell transplantation for the treatment of osteoporosis, Cell Prolif. 54 (2020), https://doi.org/10.1111/cpr.12956.
[4] S. Khosla, L.C. Hofbauer, Osteoporosis treatment: recent developments and ongoing challenges, Lancet Diabetes Endocrinol. 5 (2017) 898–907, https://doi.org/10.1016/s2213-8587(17)30188-2.

[5] J.P. Rosa, H. Raslova, M. Bryckaert, Filamin A: key actor in platelet biology, Blood 134 (2019) 1279–1288, https://doi.org/10.1182/blood.2019000014.
[6] B. Del Valle-Pérez, et al., Filamin B plays a key role in vascular endothelial growth factor-induced endothelial cell motility through its interaction with Rac-1 and Vav-2, J. Biol. Chem. 285 (2010) 10748–10760, https://doi.org/10.1074/jbc.M109.062984.
[7] T.P. Stossel, et al., Filamins as integrators of cell mechanics and signalling, Nat. Rev. Mol. Cell Biol. 2 (2001) 138–145, https://doi.org/10.1038/35052082.
[8] J.A.J. Verdonschot, et al., A mutation update for the FLNC gene in myopathies and cardiomyopathies, Hum. Mutat. 41 (2020) 1091–1111, https://doi.org/10.1002/humu.24004.
[9] S.K. Vellarikkal, et al., A founder mutation MLC1 c.736delA associated with megalencephalic leukoencephalopathy with subcortical cysts-1 in north Indian kindred, Clin. Genet. 94 (2018) 271–273, https://doi.org/10.1111/cge.13251.
[10] Q. Xu, N. Wu, L. Cui, Z. Wu, G. Qiu, Filamin B: the next hotspot in skeletal research? J Genet Genomics 44 (2017) 335–342, https://doi.org/10.1016/j.jgg.2017.04.007.
[11] G.H. Li, A.W. Kung, Q.Y. Huang, Common variants in FLNB/CRTAP, not ARHGEF3 at 3p, are associated with osteoporosis in southern Chinese women, Osteoporos. Int. 21 (2010) 1009–1020, https://doi.org/10.1007/s00198-009-1043-6.
[12] Alexander G. Baltz, et al., The mRNA-bound proteome and its global occupancy profile on protein-coding transcripts, Mol. Cell 46 (2012) 674–690, https://doi.org/10.1016/j.molcel.2012.05.021.
[13] H. Qin, et al., RNA-binding proteins in tumor progression, J. Hematol. Oncol. 13 (2020) 90, https://doi.org/10.1186/s13045-020-00927-w.
[14] M. Corley, M.C. Burns, G.W. Yeo, How RNA-binding proteins interact with RNA: molecules and mechanisms, Mol. Cell. 78 (2020) 9–29, https://doi.org/10.1016/j.molcel.2020.03.011.
[15] S. He, E. Valkov, S. Cheloufi, J. Murn, The nexus between RNA-binding proteins and their effectors, Nat. Rev. Genet. 24 (2022) 276–294, https://doi.org/10.1038/s41576-022-00550-0.
[16] I. Chepelev, G. Wei, Q. Tang, K. Zhao, Detection of single nucleotide variations in expressed exons of the human genome using RNA-Seq, Nucleic Acids Res. 37 (2009) e106, https://doi.org/10.1093/nar/gkp507.
[17] C. Trapnell, et al., Transcript assembly and quantification by RNA-Seq reveals unannotated transcripts and isoform switching during cell differentiation, Nat. Biotechnol. 28 (2010) 511–515, https://doi.org/10.1038/nbt.1621.
[18] L. Li, W. Xing, L. Jiang, D. Chen, G. Zhang, NR3C1 overexpression regulates the expression and alternative splicing of inflammation-associated genes involved in PTSD, Gene 859 (2023), https://doi.org/10.1016/j.gene.2023.147199.
[19] D.-d. Cheng, S.-j. Li, B. Zhu, S.-m. Zhou, Q.-c. Yang, EEF1D Overexpression Promotes Osteosarcoma Cell Proliferation by Facilitating Akt-mTOR and Akt-Bad Signaling, 2018, https://doi.org/10.1186/s13046-018-0715-5.
[20] C. Liang, et al., Integrin α10 regulates adhesion, migration, and osteogenic differentiation of alveolar bone marrow mesenchymal stem cells in type 2 diabetic patients who underwent dental implant surgery, Bioengineered 13 (2022) 13252–13268, https://doi.org/10.1080/21655979.2022.2079254.
[21] C. Lin, et al., PRRSV alters m(6)A methylation and alternative splicing to regulate immune, extracellular matrix-associated function, Int. J. Biol. Macromol. 253 (2023) 126741, https://doi.org/10.1016/j.ijbiomac.2023.126741.
[22] M. Hirata, et al., C/EBPβ and RUNX2 cooperate to degrade cartilage with MMP-13 as the target and HIF-2α as the inducer in chondrocytes, Hum. Mol. Genet. 21 (2012) 1111–1123, https://doi.org/10.1093/hmg/ddr540.
[23] J.M. Grewe, et al., The role of sphingosine-1-phosphate in bone remodeling and osteoporosis, Bone Research 10 (2022), https://doi.org/10.1038/s41413-022-00205-0.
[24] J.Q. Ng, et al., Loss of Grem1-lineage chondrogenic progenitor cells causes osteoarthritis, Nat. Commun. 14 (2023) 6909, https://doi.org/10.1038/s41467-023-42199-1.
[25] X. Luo, et al., Vascular NRP2 triggers PNET angiogenesis by activating the SSH1-cofilin axis, Cell Biosci. 10 (2020) 113, https://doi.org/10.1186/s13578-020-00472-6.
[26] D. Dubey, et al., Identification of caveolae-associated protein 4 autoantibodies as a biomarker of immune-mediated rippling muscle disease in adults, JAMA Neurol. 79 (2022), https://doi.org/10.1001/jamaneurol.2022.1357.
[27] C. Niehrs, C.F. Calkhoven, Emerging role of C/EBPβ and epigenetic DNA methylation in ageing, Trends Genet. 36 (2020) 71–80, https://doi.org/10.1016/j.tig.2019.11.005.
[28] S. Muruganandan, A.M. Ionescu, C.J. Sinal, At the crossroads of the adipocyte and osteoclast differentiation programs: future therapeutic perspectives, Int. J. Mol. Sci. 21 (2020) 2277, https://doi.org/10.3390/ijms21072277.
[29] J.R. Harrison, et al., Col1a1 promoter-targeted expression of p20 CCAAT enhancer-binding protein beta (C/EBPbeta), a truncated C/EBPbeta isoform, causes osteopenia in transgenic mice, J. Biol. Chem. 280 (2005) 8117–8124, https://doi.org/10.1074/jbc.M410076200.
[30] V.V. Iyer, T.B. Kadakia, L.R. McCabe, R.C. Schwartz, CCAAT/enhancer-binding protein-β has a role in osteoblast proliferation and differentiation, Exp. Cell Res. 295 (2004) 128–137, https://doi.org/10.1016/j.yexcr.2004.01.004.
[31] D.L. Worthley, et al., Gremlin 1 identifies a skeletal stem cell with bone, cartilage, and reticular stromal potential, Cell 160 (2015) 269–284, https://doi.org/10.1016/j.cell.2014.11.042.
[32] D.P. Brazil, R.H. Church, S. Surae, C. Godson, F. Martin, BMP signalling: agony and antagony in the family, Trends Cell Biol. 25 (2015) 249–264, https://doi.org/10.1016/j.tcb.2014.12.004.
[33] E. Hanaoka, et al., Overexpression of DAN causes a growth suppression in p53-deficient SAOS-2 cells, Biochem. Biophys. Res. Commun. 278 (2000) 20–26, https://doi.org/10.1006/bbrc.2000.3758.
[34] B. Chen, M. Athanasiou, Q. Gu, D.G. Blair, Drm/Gremlin transcriptionally activates p21(Cip1) via a novel mechanism and inhibits neoplastic transformation, Biochem. Biophys. Res. Commun. 295 (2002) 1135–1141, https://doi.org/10.1016/s0006-291x(02)00828-8.
[35] Y. Zhang, Q. Zhang, Bone morphogenetic protein-7 and Gremlin: new emerging therapeutic targets for diabetic nephropathy, Biochem. Biophys. Res. Commun. 383 (2009) 1–3, https://doi.org/10.1016/j.bbrc.2009.03.086.
[36] H. Li, et al., ZIP10 drives osteosarcoma proliferation and chemoresistance through ITGA10-mediated activation of the PI3K/AKT pathway, J. Exp. Clin. Cancer Res. 40 (2021) 340, https://doi.org/10.1186/s13046-021-02146-8.
[37] Y. Song, et al., miR-4739/ITGA10/PI3K signaling regulates differentiation and apoptosis of osteoblast, Regenerative Therapy 21 (2022) 342–350, https://doi.org/10.1016/j.reth.2022.08.002.
[38] M.R. King, S. Petry, Phase separation of TPX2 enhances and spatially coordinates microtubule nucleation, Nat. Commun. 11 (2020), https://doi.org/10.1038/s41467-019-14087-0.
[39] C. Cai, et al., Transcriptional and open chromatin analysis of bovine skeletal muscle development by single-cell sequencing, Cell Prolif. 56 (2023), https://doi.org/10.1111/cpr.13430.
[40] P. Vrtačnik, et al., Epigenetic enzymes influenced by oxidative stress and hypoxia mimetic in osteoblasts are differentially expressed in patients with osteoporosis and osteoarthritis, Sci. Rep. 8 (2018) 16215, https://doi.org/10.1038/s41598-018-34255-4.
[41] V.L. Ruiz-Perez, et al., Evc is a positive mediator of Ihh-regulated bone growth that localises at the base of chondrocyte cilia, Development 134 (2007) 2903–2912, https://doi.org/10.1242/dev.007542.
[42] M. Saito, et al., Cytoskeletal protein 4.1G is essential for the primary ciliogenesis and osteoblast differentiation in bone formation, Int. J. Mol. Sci. 23 (2022), https://doi.org/10.3390/ijms23042094.
[43] C.A. Liu, M.J. Wang, C.W. Chi, C.W. Wu, J.Y. Chen, Rho/Rhotekin-mediated NF-kappaB activation confers resistance to apoptosis, Oncogene 23 (2004) 8731–8742, https://doi.org/10.1038/sj.onc.1208106.
[44] Z. Li, et al., A comprehensive overview of PPM1B: from biological functions to diseases, Eur. J. Pharmacol. 947 (2023) 175633, https://doi.org/10.1016/j.ejphar.2023.175633.